

CHARACTERIZATION OF POLYSACCHARIDE-ESSENTIAL OIL BIODEGRADABLE COATINGS. APPLICATION TO TOMATO FRUIT

Presented by: Alina Tampau

Academic directors: Maria Desamparados Vargas Colas, Lorena Atares Huerta¹

RESUMEN

Se prepararon películas biodegradables utilizando quitosano o metilcelulosa con aceites esenciales (AE) de albahaca, tomillo u orégano. El tamaño de las partículas y las propiedades reológicas de las dispersiones formadoras de película (DFPs) fueron estudiados. Las películas se acondicionaron (25 °C - 53 % HR) y se analizó su microestructura, permeabilidad al vapor de agua, contenido de humedad y pérdida de aceite esencial. Las películas a base de quitosano mostraron una mejor integración y retención de los AE en la matriz. Se llevaron a cabo pruebas *in vitro* del poder antifúngico de los AE, con *Botrytis cinerea* y *Rhizopus stolonifer*. Los AE de tomillo y orégano presentaron la actividad antifúngica más fuerte, mientras que el de albahaca demostró la inhibición más débil. DFPs con AE de tomillo fueron rociadas sobre los frutos de tomate (cv. Micro-Tom), que después se recogieron estando verdes o maduros. La tasa de respiración, evolución del color, contenido en sólidos solubles, pH y acidez titulable se evaluaron durante el almacenamiento. Los frutos recubiertos con DFPs a base de metilcelulosa enrojecieron primero. El patrón de la respiración no se vio afectado por la aplicación del recubrimiento.

Palabras clave: Recubrimiento comestible, quitosano, metilcelulosa, aceite esencial de albahaca, aceite esencial de tomillo, aceite esencial de orégano, antifúngico

RESUM

Es van preparar pel·lícules biodegradables utilitzant quitosan o metilcel·lulosa amb olis essencials (OE) d'alfàbrega, farigola o orenga. La mida de les partícules i les propietats reològiques de les dispersions formadores de pel·lícula (DFPs) van ser estudiats. Les pel·lícules es van condicionar (25 °C - 53% HR) i es van analitzar la seva microestructura, permeabilitat al vapor d'aigua, contingut d'humitat i pèrdua d'oli essencial. Les pel·lícules a força de

¹ Instituto Universitario de Ingeniería de Alimentos para el Desarrollo, Universidad Politécnica de Valencia, camino de Veras/n. 46022, Valencia, Spain.

Tel. +34 963877056 • Fax +34 963877956 • e-mail: iad@iad.upv.es • www.iad.upv.es

quitosa mostraren una millor integració i retenció dels OE en la matriu. Proves antifúngics *in vitro* es van dur a terme amb *Botrytis cinerea* i *Rhizopus stolonifer*. Els OE de farigola i orenga presentaren l'activitat antifúngica més forta, mentre que el de alfàbrega va demostrar la inhibició més feble. Dispersions amb OE de farigola van ser ruixades sobre els fruits de tomàquet (cv. Micro - Tom), que després es van recollir estant verds o madurs. La taxa de respiració, evolució del color, contingut en sòlids solubles, pH i acidesa titulable es van avaluar durant l'emmagatzematge. Els fruits recoberts amb DFPs a base de metilcel·lulosa es van enrogir primer. El patró de la respiració no es va veure afectat per l'aplicació del recobriment.

Paraules clau: Recobriment comestible, el quitosan, metil cel·lulosa, oli essencial d'alfàbrega, oli essencial de farigola, oli essencial d'orenga, antifúngic

ABSTRACT

Biodegradable films were prepared using chitosan or methylcellulose with basil, thyme or oregano essential oils. The rheological properties and particle size of the film-forming dispersions (FFDs) were studied. The films were conditioned (25°C-53% RH) and analyzed for their microstructure, water vapor permeability, moisture content and essential oil loss. Chitosan-based films showed better integration and retention of the essential oils in the matrix. *In vitro* antifungal tests were performed with *Botrytis cinerea* and *Rhizopus stolonifer*. Thyme and oregano essential oils presented the strongest antifungal activity, while basil essential oil showed the weakest inhibition. Thyme essential oil dispersions were sprayed on tomato fruits (cv. Micro-tom) and were harvested at green or ripe stages. The respiration rate, color evolution, soluble solids content, pH and titrable acidity were evaluated during storage. The fruits coated with methylcellulose-based FFDs became red first. The respiration pattern was not affected by coating application.

Keywords: Edible coating, chitosan, methylcellulose, basil essential oil, thyme essential oil, oregano essential oil, antifungal

1. INTRODUCTION

There is growing consumer awareness about the pesticides and herbicides employed in the cultivars. The demand for healthy foods is encouraging organic and environmentally-friendly plant treatments. In this sense, alternative methods to treat fruits and vegetable have started to be explored [Angelini et al., (2003)].

An interesting focus is on essential oils (EO), as they are natural antioxidant and antimicrobial lipidic substances extracted from herbs and spices [Bakkali et al., (2008)]. Most of them consist of a mixture of terpens, terpenoids and other aromatic and aliphatic constituents, but their composition can vary depending on the specific oil. Remarkable concentrations of carvacrol (46.1%), thymol (25.6%),

γ -terpinen (10.5%) and p-cymene (7.5%) are detected in oregano EO, while β -linalool (44.2%), p-menth-1-en-4-ol (14.2%), p-cymene (5.2%) and borneol (3.5%) are abundant in thyme EO. 1-methoxy-4-(w-propenyl)-benzene (55.0%) and eucalyptol (26.4%) appeared as the main compounds of basil EO. All these compounds lead to the EO strong antioxidant properties [Lee et al., (2005); Sari et al., (2006)].

Treatments with EO and polysaccharides emulsions result in edible-level coatings that protect and extend the shelf life [Pedones et al. (2012)]. Methyl cellulose and chitosan are among the preferred matrixes for incorporating the EO in emulsions, due to their natural origin and biodegradability.

Methylcellulose is a cellulose (poly- β -(1 \rightarrow 4)-D-glucopyranose) derivative, formed by the alkali treatment of cellulose, followed by a reaction with methyl chloride. MC is stable at a wide range of pH (2–11) and exhibits high solubility, and efficient oxygen and lipid barrier properties [Turhan and Sahboz, (2004)].

Chitosan, a hydrophilic linear β -(1,4)-glucosamine polymer obtained by N-deacetylation of chitin, is also a known antimicrobial agent against fungi, bacteria, and viruses [Kim et al., (2005)].

Tomato (*Lycopersicon esculentum*) is one of the most widely spread horticultural crops in the world [Polder et al., (2010)]. During ripening of fruit, the cell wall begins to soften due to the activity of certain enzymes that alter its texture, by degradation of structural components necessary to reinforce the cell wall and the adhesion of cells. This behavior makes the fruit more susceptible to the post-harvest attack of diseases, especially moulds. *Rhizopus sp.* and *Botrytis sp.* are the most prevalent attackers (the latter especially in Mediterranean greenhouses [Baptista et al., (2012)] causing progressive deterioration of the tomatoes. The Micro-tom cultivar was used due to its small size and rapid growth, which recommend it as a convenient plant model for research.

The aim of this work was to characterize the physicochemical and antimicrobial properties of applied EO-polysaccharide films and evaluate their effect on tomato fruit in terms of changes in respiration rate and physicochemical characteristics during post-harvest storage.

2. MATERIALS AND METHODS

2.1. Reagents and raw materials

High molecular weight chitosan (CH), with a deacetylation degree of 75.6% (CAS Number 9012-76-4, Batch MKBG8530V, Sigma–Aldrich, USA, viscosity in 0.5% (wt) glacial acetic acid solution: 1.406 Pa s), 98% glacial acetic acid, and **Methylcellulose (MC)** (Batch 72757, VWR BDH Prolabo, viscosity in 2.0% (wt) water solution: 400 mPa s) are used as matrixes for the coatings. **Thyme (T)** (*Thymus vulgaris* L.) (Batch A5753), **Basil (B)** (*Ocimum basilicum* L.) (Batch A1906) and **Oregano (O)** (*Origanum vulgare* L.) (Batch A3490) EOs

were provided by Herbes del Moli (Benimarfull, Alicante, Spain). **Tween 85** (Batch 1262745) was provided by Fluka and **silicone** (Batch 0000147416) by Panreac.

Tomato (*Lycopersicon esculentum*) plants (cultivar Micro-Tom) grown in greenhouse conditions (ETSIAMN, UPV) were used for the coating application experiments. A total of 10 plants per formulation were used, while reserving 10 plants as untreated controls.

The molds used were *Rhizopus stolonifer* (CECT 2344) and *Botrytis cinerea* (CECT 20516), both supplied by Colección Española de Cultivos Tipo (CECT, Burjassot, Spain).

2.2. Preparation and characterization of the film-forming dispersions (FFD)

CH (0.5%, w/w) was dispersed in an aqueous solution of glacial acetic acid (0.5%, v/w). MC (0.5% w/w) was dispersed in distilled water and heated up to 80°C for 10 minutes with continuous stirring. After the polysaccharides were dissolved, EOs were added to reach a final concentration of 0.25% (w/w) along with 0,01% (w/w) Tween 85 and 1 drop of silicone (as anti-foaming agent only for the MC dispersions) The mixtures were emulsified using a rotor–stator homogenizer (Model T25D, Ika Germany) at 12,000 rpm for 4 min. These FFDs were designated as CH, CH+T, CH+B, CH+O, MC, MC+T, MC+B and MC+O.

2.2.1. PARTICLE SIZE MEASUREMENTS

Particle size measurements of the FFDs were performed using a laser diffractometer (Mastersizer, 2000; Malvern Instruments, Worcestershire, UK) with ultrasound application. The dispersion was added at 1950 rpm until an obscuration rate of 8% was obtained. The MC based formulas were dispersed in distilled water, while the CH based samples were diluted in 800mL deionized water with 10 μ L glacial acetic acid added, to imitate the solvent. Triple measurement per formulation was made. The volume-surface mean diameter ($d_{3,2}$) and the weight mean diameter ($d_{4,3}$) [Atarés et al., (2010)] as well as the droplet size distribution were determined.

2.2.2. RHEOLOGICAL BEHAVIOR

The rheological behavior of FFDs was analyzed in triplicate at 25°C using a rotational rheometer (HAAKE Rheostress 1, Thermo Electric Corporation, Karlsruhe, Germany) with a sensor system of coaxial cylinders, type Z34DIN Ti. Samples were left to rest for 5 min before the measurements were taken. The shear stress (σ) was obtained as a function of shear rate ($\dot{\gamma}$) between 0 and 512 s⁻¹, taking 5 min for each (ramp up and down) cycle. Experimental data were

fitted to the Ostwald de Waale model (equation (1)) in order to determine the consistency (K) and the flow behavior indexes (n).

$$\sigma = K \cdot \dot{\gamma}^n \quad (1)$$

where: σ = shear stress (Pa); K = flow consistency index (Pa·sⁿ); $\dot{\gamma}$ = shear rate (s⁻¹); n = flow behavior index.

2.3. Preparation and characterization of the stand-alone films

2.3.1. CASTING, DRYING AND CONDITIONING

The FFDs were cast on Teflon® plates of 15cm diameter to form dry films with 56.65 g solids/m². After four days at 45 (±2)% relative humidity (RH) and 25°C, the dry films were conditioned for a week in desiccators at 25°C and 53% RH, generated by using oversaturated magnesium nitrate solution (Batch 0000434152, Panreac, Barcelona, Spain).

2.3.2. THICKNESS

Film thickness was determined with a Palmer digital micrometer (Comecta, Barcelona, Spain) to the nearest 0.001 mm. Five measurements per film were done and the average value was used in water vapor permeability (WVP) calculations.

2.3.3. MICROSTRUCTURE

Microstructure was analyzed by SEM in cross-sectioned cryofractured film specimens, using a JEOL JSM-5410 (Japan) electron microscope. The film samples were previously equilibrated with P₂O₅ (Panreac, Barcelona, Spain) for at least 30 days to eliminate water. Once dehydrated, they were cryofractured by immersion in liquid nitrogen and mounted on metallic stubs perpendicularly to their surface. After gold coating, the images were captured using an accelerating voltage of 10 kV.

2.3.4. EQUILIBRIUM MOISTURE CONTENT AND WATER VAPOR PERMEABILITY

The water vapor permeability (WVP) was determined in quadruplicate for each film formula, using polymethylmethacrylate "Payne" cups following the design proposed by Gennadios, Weller, and Gooding (1994). Deionised water was used inside the testing cup to achieve 100% RH on one side of the film, while an oversaturated magnesium nitrate solution was used to achieve 53% RH on the outer side of the film. The preconditioned films were cut into 6 cm

diameter circles and placed on the cups. The side that was in contact with the PTFE plate during drying was placed towards the highest RH. This was done to simulate that FFD is applied and dries on the surface of the plant and its fruit. A fan placed on the top of the cup was used to promote convection. Water vapor transmission rate measurements (WVTR) were performed at 25°C to reproduce the storage conditions of the coated products. To calculate WVTR, the slopes of the steady state period of the curves of weight loss as a function of time were determined by linear regression. The WVP was determined from WVTR values, as described by equation 2.

$$WVP = \frac{WVTR}{P_{w1} - P_{w2}} \cdot L \quad (2)$$

where: WVTR = water vapor transmission rate ($\text{g}\cdot\text{h}^{-1}\cdot\text{m}^{-2}$); P_{w1} = partial pressure of water vapor on the film's underside (Pa); P_{w2} = partial pressure of water on the film's upper surface (Pa); L = film thickness (m).

2.3.5. ESSENTIAL OIL LOSS IN FILMS

The weights of FFDs and films were registered at pouring, after drying, after humidity was balanced (25°C / 53%RH for 7 days) and finally after dehydration with P_2O_5 (25°C for at least 30 days). The residual EO content was calculated using a simple mass balance, subtracting from the weight of the balanced film the weight of the corresponding polymer, Tween 85 and/or silicone and the water content. It was assumed that water is the only component that the films lose when placed in the P_2O_5 environment. The loss of EO was expressed as a percentage compared to the initial EO poured with the FFD.

2.3.6. IN VITRO ANTIFUNGAL TESTS

Fungal strains were kept frozen (-25°C) in Potato Dextrose Agar (Scharlab, Barcelona, Spain) supplemented with 30% glycerol (Panreac, Barcelona, Spain). Fungi were inoculated on potato dextrose agar (PDA) and incubated at 25°C until sporulation. The spores were counted in a Thoma counting chamber and diluted to a concentration of 10^3 spores/plate ($18 \text{ spores}/\text{cm}^2$).

The diluted spore solution was inoculated on the surface of Petri dishes containing PDA. To perform the inhibition halo tests, sterile paper disks (20mm in diameter) were placed on the inoculated PDA surfaces (direct contact & volatility test) or in the lid of the Petri dish (volatility test). The disks were impregnated with 30 μL aliquot of EO-dimethylsulfoxide (DMSO, Batch 0000339164, Panreac) solutions (0%, 0.25%, 0.5%, 1.0% and 2.0% (w/v)). Plates were then sealed with parafilm to avoid dehydration and stored for 11 days at 25°C.

The test was performed in triplicate for each EO concentration and fungal strain. One representative plate per EO concentration and mold strain was selected and analyzed in triplicate for its degree of sporulation. Selected plates were flooded with 20mL of physiologic serum (PS) (7% NaCl and 0.01% Tween 85 in distilled water) and their surface was scraped to release the spores. An aliquot of 1mL of this suspension was diluted with 9 mL PS and observed with the Thoma chamber.

2.4. Application on tomato fruits

Film-forming dispersions were applied to tomato plants at the stage of green fully formed fruits by using 1 L pressure sprayers (Menan, Valencia). Two sample groups of tomatoes were analyzed over post-harvest storage at 25°C and 53% RH. One group of samples consisted of green unripe fruits harvested 7 days after the coating application. The other group was ripe red fruits harvested 23 days after coating application.

2.4.1. ACIDITY, pH, SOLUBLE SOLIDS AND MATURITY INDEX

The fruits were ground with an Ultraturax at 12000 rpm for 4 min. The pH, acidity and soluble solids (Brix) determinations were all done in triplicate. Measurement of pH was carried out by means of a pH-meter (GLP 21+, Crison, Barcelona, Spain). Acidity was analyzed following a modified version of method AOAC 942.15 (AOAC, 1995), and was expressed as g of citric acid per 100 g of fruit. Total soluble solids were measured as Brix by means of a 3 T ABBE refractometer (ATAGO Co Ltd., Japan) at 20°C. The maturity index was calculated as a quotient between soluble solids (Brix) and acidity.

2.4.2. RESPIRATION RATE

Tomatoes were placed in 0.940 L hermetic glass jars with a septum in the lid for sampling the gas in the headspace at different times. The jars were stored in a climate chamber at 25°C. Gas sampling was carried out every 60-120 min by means of a needle connected to a gas analyzer (CheckMate 9900 PBI Dansensor, Ringsted, Denmark). Two replicates per treatment were performed.

2.4.3. COLOR PROGRESSION OVER STORAGE

The color progression was evaluated using a CM-3600d spectrophotometer (Minolta Co, Tokyo, Japan) with a 10 mm diameter window. The measurements were carried out daily for 14 days in 5 samples per treatment. CIE L*a*b* coordinates, hue (h_{ab}^*) and chroma (C_{ab}^*) (CIE, 1986) were obtained from the reflection spectra of the samples using D65 illuminant and 10° observer.

3. RESULTS AND DISCUSSION

3.1. Preparation and characterization of the film-forming dispersions

3.1.1. PARTICLE SIZE MEASUREMENT

The particle size distribution of the FFDs is shown in figure 1, and table 1 shows the values of mean size $d_{3,2}$ (surface) and $d_{4,3}$ (volume).

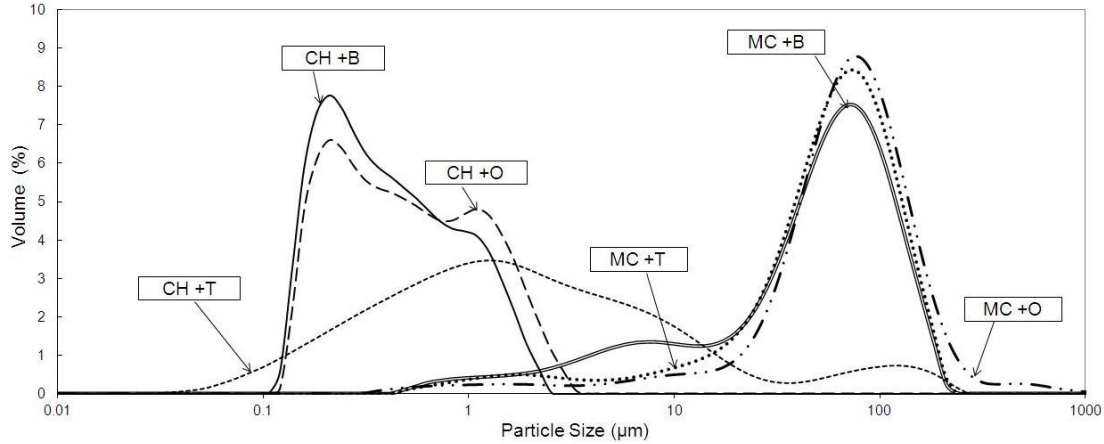


FIGURE 1. Particle size distribution in terms of volume of FFDs with basil (B), thyme (T) and oregano (O) essential oils, at 0.25% (p/p) in the FFD.

TABLE 1. Average diameter $d_{3,2}$, $d_{4,3}$ in size distributions, apparent viscosity at 100 s^{-1} and 500 s^{-1} , consistency (K) and flow behavior indexes (n). Average values and standard deviations, in brackets.

FFD	$d_{3,2}$ (μm)	$d_{4,3}$ (μm)	K ($\text{mPa}\cdot\text{s}^n$)	n	μ_{ap}^{100} ($\text{mPa}\cdot\text{s}$)	μ_{ap}^{500} ($\text{mPa}\cdot\text{s}$)
CH	-	-	79.4(1.4) ^f	0.862(0.004) ^a	42.15(0.06) ^e	58(14) ^b
CH+T	0.77(0.14) ^a	14(6) ^b	70.4(0.9) ^e	0.868(0.002) ^{ab}	38.5(0.2) ^d	60.81(0.17) ^b
CH+B	0.405(0.002) ^a	0.673(0.004) ^a	104.3(1.6) ^g	0.836(0.002) ^a	49.1(0.4) ^f	73.7(0.4) ^c
CH+O	0.464(0.002) ^a	0.846(0.003) ^a	46.26(1.03) ^d	0.920(0.004) ^b	32.1(0.3) ^c	55.1(0.4) ^b
MC	-	-	3.35(0.04) ^{ab}	1.14(0.09) ^d	7(3) ^b	-
MC+T	18.2(0.7) ^c	81.5(0.6) ^d	4.76(0.04) ^{bc}	1.0789(0.0009) ^c	6.84(0.03) ^b	15.17(0.04) ^a
MC+B	14.8(1.9) ^b	73(3) ^c	5.11(0.08) ^c	1.072(0.002) ^c	7.11(0.07) ^b	15.50(0.13) ^a
MC+O	22.85(1.13) ^d	106.3(1.5) ^e	2.920(0.107) ^a	1.047(0.004) ^c	3.63(0.03) ^a	-

Different superscripts (a, b and c) indicate significant differences according to ANOVA test ($p < 0.05$).

Distributions were mostly unimodal and, compared to the MC formulations, the CH ones present reduced particle sizes for both surface and volume values. This could be explained by a better response of the CH-based FFDs to the homogenization process. In fact, CH is considered as a polymeric surfactant that yields stable water-in-oil emulsions by promoting electrosteric stabilization mechanisms [Rodríguez et al., (2002)]. The type of essential oil seems to affect $d_{3,2}$ and $d_{4,3}$. In the case of CH films, CH+T presents the biggest diameter values,

while for MC films, MC+O displays the highest values. The specific interactions between the components of the essential oils and the polysaccharides would explain the differences caused by the EO added.

3.1.2. RHEOLOGICAL BEHAVIOR

The experimental values for the K and n indexes are presented in table 1, and the flow curves are represented in figure 2.

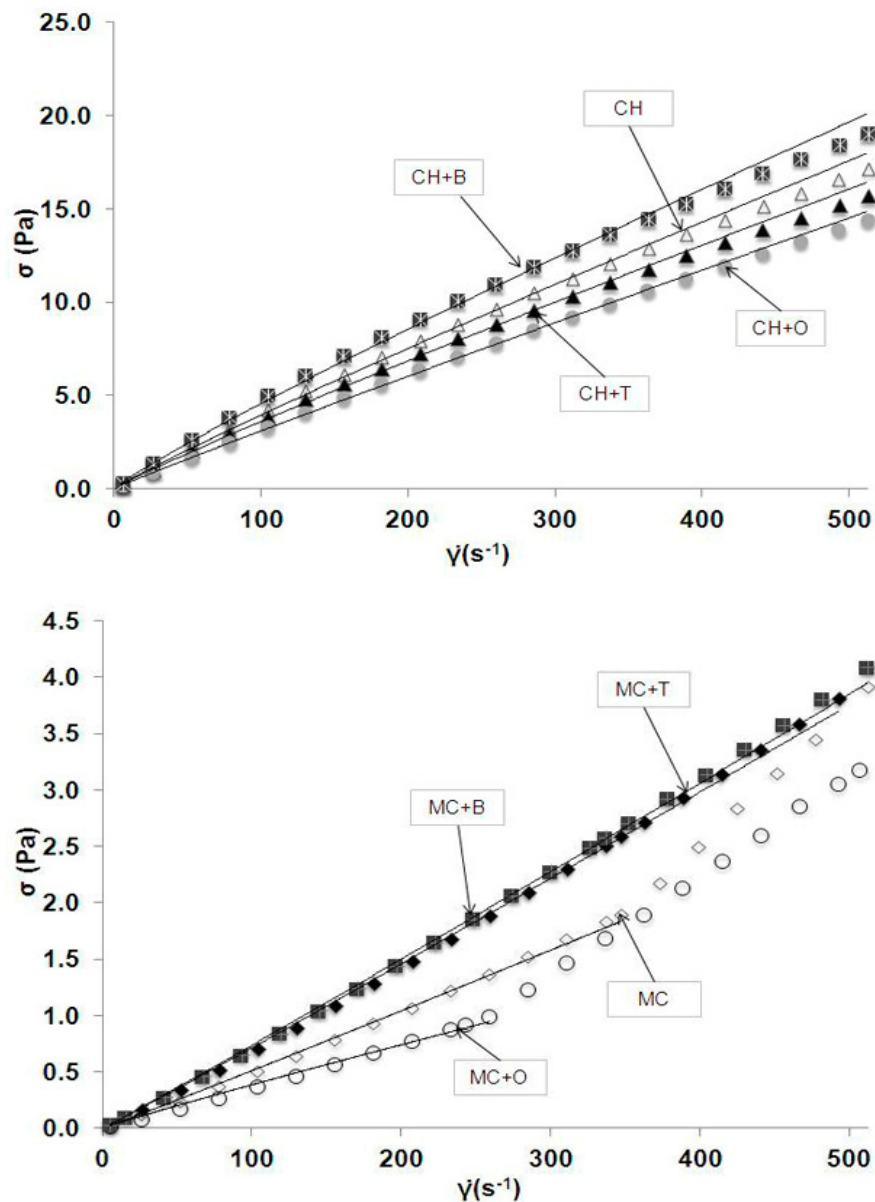


FIGURE 2. Flow curves of CH (top) and MC (bottom) based FFDs

All CH FFDs fitted the model closely up to 512s^{-1} and showed shear thinning behavior. The smaller the particle size, the more surface area is present, which generates increased friction between molecules and a higher viscosity.

The same trend was observed by Ahmed et al (2014) in flour dispersions. MC+B and MC+T experimental data fitted the model closely for the entire velocity gradient range ($0\text{-}512\text{s}^{-1}$), whereas MC and MC+O only did so up to 346s^{-1} and 258s^{-1} respectively. The behavior of all MC FFDs was mainly Newtonian, with average n values ranging between 1.047 and 1.138. Similar results were obtained by Song et al., (2010).

3.2. Characterization of the stand-alone films

3.2.1. MICROSTRUCTURE

Figure 3 shows the SEM-micrographs of the films cross-sections.

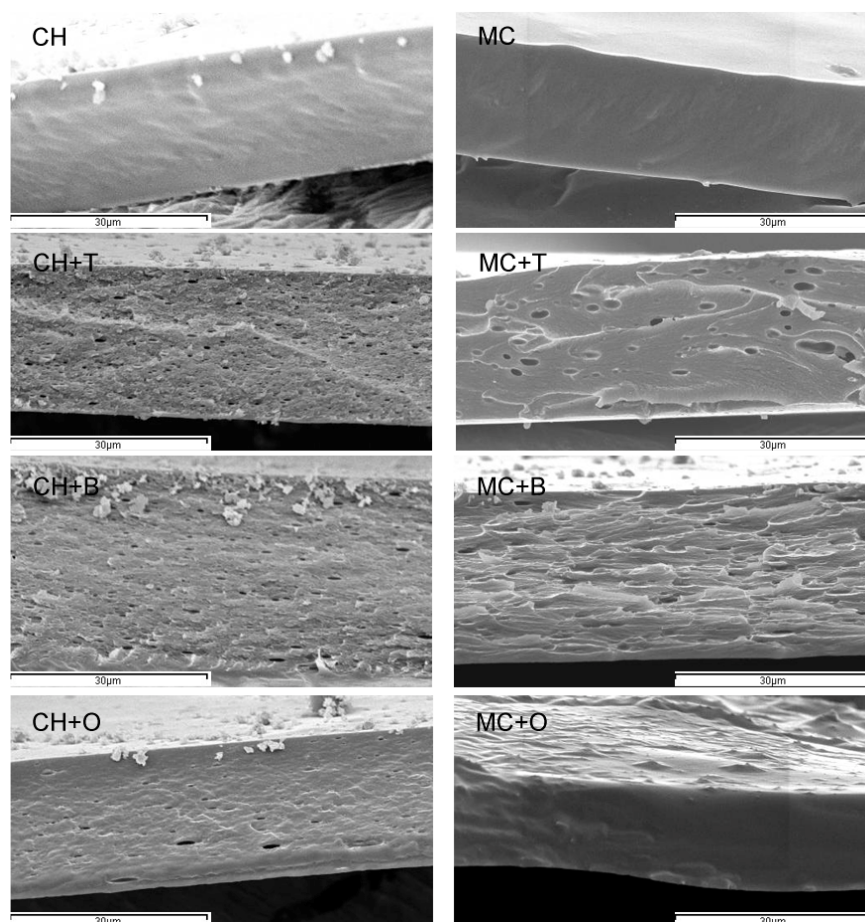


FIGURE 3. Scanning Electron Microscopy (SEM) micrographs of the films cross sections

The different droplet size distribution in the FFD influences the final microstructure of the stand-alone films. Films without EO showed a homogenous structure, without visible irregularities. Coherently with the size distribution of the FFD, the droplets in CH+EO films were smaller as compared to MC+EO films. In addition, the films prepared with CH presented a better integration of the EO in the film matrix.

3.2.2. EQUILIBRIUM MOISTURE CONTENT, WATER VAPOR PERMEABILITY AND ESSENTIAL OIL LOSS

The data collected for equilibrium moisture content (EMC) and water vapor permeability (WVP) are presented in table 2.

TABLE 2. Equilibrium moisture content (EMC) (g water/100 g moist film) of films stored at 53%RH, water vapor permeability (WVP) at 25° and 53-100%RH (g Pa⁻¹ s⁻¹ m⁻¹) and EO loss (g lost EO/100 g initial EO in the FFD) of the stand-alone films. Average values and standard deviations, in brackets.

Film	EMC (%)	WVP·10 ¹¹ (g·Pa ⁻¹ ·s ⁻¹ ·m ⁻¹)	EO loss (%)
CH	9.6(0.2) ^d	105(10) ^d	-
CH+T	9.3(0.4) ^{cd}	96(15) ^{cd}	40.4(0.9) ^a
CH+B	9.12(0.15) ^{cd}	105(11) ^d	46.142 (1.007) ^a
CH+O	8.99(0.12) ^c	96(36) ^{cd}	46.66(1.13) ^a
MC	1.5(0.8) ^b	74(8) ^{bc}	-
MC+T	0.87(0.19) ^a	42(13) ^a	84.7(0.5) ^b
MC+B	0.9(0.2) ^a	55(2) ^{ab}	88.1(0.7) ^b
MC+O	1.3(0.4) ^{ab}	71(18) ^b	76.02(0.02) ^c

Different superscripts (a, b and c) indicate significant differences according to ANOVA test (p < 0.05).

MC films presented significantly lower EMC values than CH films (p<0.05) at the same storage. This is due to the strong hydrophilic character of CH as compared to MC, as previously reported by Vargas et al., (2011). The inclusion of EOs in the polysaccharides structure brings a slight descend of the moisture content for both matrixes, which is due to the substitution of part of the polymer by a hydrophobic compound.

CH films exhibit higher WVP than those formulated with MC, consistent with previous results [Garcia et al., (2004)]. The addition of EOs slightly increased the films hydrophobicity and modified their barrier properties, lowering the WVP. Thyme EO was the most effective in lowering WVP.

The data for EO losses are shown in table 2. The higher losses were obtained for MC-based films for all incorporated EO. It seems that the determining factor in EO loss is the nature of the polymer matrix and not the type of EO. The losses for chitosan-EO films are in the range to that reported by Sánchez-González et al. (2011) in CH-bergamot essential oil films at the same CH:EO ratio.

It seems that CH is more effective at encapsulating EO than MC. This is coherent with the microstructure of the cross-sections of the films, which proved a more homogenous EO droplet incorporation in the CH structures.

3.2.3. IN VITRO ANTIFUNGAL TESTS

Results of the *in vitro* tests performed with EOs solutions on *Botrytis cinerea* and *Rhizopus stolonifer* are shown in tables 3 and 4, respectively.

TABLE 3. Antifungal activity of EOs on *B. cinerea* expressed as % of inhibition area. (*) no changes with respect to the previous measurement time.

days	B (g/100ml DMSO)				T (g/100ml DMSO)				O (g/100ml DMSO)			
	0.25	0.5	1.0	2.0	0.25	0.5	1.0	2.0	0.25	0.5	1.0	2.0
total effect on vegetative growth												
2	11.7	31.6	58.2	100	4.9	100	100	100	81.5	100	100	100
3	9.6	21.1	24.5	(*)	(*)	42.5	76.8	(*)	(*)	(*)	(*)	(*)
4	4.9	10.4	16.1	26.6	(*)	(*)	50.0	(*)	78.8	(*)	(*)	(*)
7	(*)	4.9	5.3	8.6	4.0	22.1	24.4	(*)	75.9	(*)	(*)	(*)
11	0.0	(*)	4.9	4.9	3.6	12.6	4.9	(*)	75.5	(*)	(*)	(*)
volatility-only effect on vegetative growth												
2	0.0	0.0	0.0	100	3.8	100	100	100	67.4	57.8	100	100
3	(*)	(*)	(*)	(*)	3.8	(*)	(*)	(*)	64.8	(*)	(*)	(*)
4	(*)	(*)	(*)	4.7	1.6	59.2	(*)	(*)	(*)	(*)	84.2	87.5
7	(*)	(*)	(*)	0.0	0.0	45.8	(*)	(*)	(*)	(*)	(*)	(*)
11	(*)	(*)	(*)	(*)	(*)	13.0	(*)	(*)	60.1	(*)	(*)	(*)
total effect on sporulation												
4	100	100	100	100	100	100	100	100	100	100	100	100
7	(*)	36.6	(*)	63.7	68.0	36.6	100	(*)	(*)	(*)	(*)	(*)
9	(*)	(*)	4.9	(*)	67.7	(*)	38.1	(*)	(*)	(*)	(*)	(*)
11	0.0	(*)	(*)	17.8	(*)	23.1	20.8	(*)	(*)	(*)	(*)	(*)
volatility-only effect on sporulation												
4	100	100	100	100	100	100	100	100	100	100	100	100
7	0.0	0.0	33.3	0.0	0.0	(*)	(*)	(*)	(*)	(*)	(*)	(*)
9	(*)	(*)	(*)	(*)	(*)	56.1	(*)	(*)	(*)	(*)	(*)	(*)
11	(*)	(*)	(*)	(*)	(*)	34.3	(*)	(*)	(*)	(*)	(*)	(*)

The evolution over time of the inhibition effect has a descending trend, with a maximum antifungal response being registered at two days. As expected, increased percentages of EOs led to a stronger antifungal activity (higher inhibition halo). Basil EO had the least effect on fungal development, although it led to a delay in the sporulation of *R. stolonifer* when added at 0.25%. Thyme and oregano EO at the highest concentration (2%) inhibited completely both vegetative growth and sporulation of *B. cinerea*. Thyme and oregano EO led to a significant delay of sporulation (of at least 4 days) for both fungi. Taking into account these results, basil EO was rejected to perform the *in vivo* treatments with the FFDs. Taking to account that the FFDs would be applied in the greenhouse, thyme EO was selected for its high volatile effect. The lowest EO concentration (0.25% p/p) was preferred in order to prevent likely phytotoxicity.

TABLE 4. Antifungal activity of EO on *R. stolonifer* strain expressed as % of inhibition area. (*) no changes with respect to the previous measurement time.

B (g/100ml DMSO)					T (g/100ml DMSO)				O (g/100ml DMSO)			
total effect on vegetative growth												
%	0.25	0.5	1.0	2.0	0.25	0.5	1.0	2.0	0.25	0.5	1.0	2.0
2	0.0	3.5	4.7	2.8	0.0	5.3	22.9	72.9	47.4	68.1	57.4	74.6
3	(*)	(*)	(*)	0.0	(*)	4.7	11.7	(*)	46.5	67.9	(*)	(*)
4	(*)	0.0	0.0	(*)	(*)	(*)	4.2	63.6	46.0	(*)	(*)	(*)
7	(*)	(*)	(*)	(*)	(*)	0.0	0.0	58.2	43.9	(*)	(*)	(*)
11	(*)	(*)	(*)	(*)	(*)	(*)	(*)	50.0	13.1	58.0	(*)	(*)
volatility-only effect on vegetative growth												
%	0.25	0.5	1.0	2.0	0.25	0.5	1.0	2.0	0.25	0.5	1.0	2.0
2	0.0	0.0	0.0	0.0	0.0	0.1	6.2	14.6	30.0	27.5	30.2	38.2
3	(*)	(*)	(*)	(*)	(*)	(*)	3.6	8.6	21.5	26.4	29.9	38.1
4	(*)	(*)	(*)	(*)	(*)	0.0	0.2	6.2	4.5	17.7	(*)	(*)
7	(*)	(*)	(*)	(*)	(*)	(*)	(*)	(*)	(*)	(*)	8.4	25.8
11	(*)	(*)	(*)	(*)	(*)	(*)	0.0	0.0	0.0	0.0	0.0	13.7
total effect on sporulation												
%	0.25	0.5	1.0	2.0	0.25	0.5	1.0	2.0	0.25	0.5	1.0	2.0
4	43.2	53.5	26.6	74.4	0.4	33.9	53.5	100	100	100	100	100
7	3.5	33.6	1.4	33.7	0.0	33.3	0.0	66.7	77.5	(*)	(*)	(*)
9	2.4	33.3	0.0	33.3	(*)	(*)	(*)	(*)	66.7	(*)	(*)	(*)
11	2.1	(*)	(*)	(*)	(*)	(*)	(*)	(*)	(*)	(*)	(*)	(*)
volatility-only effect on sporulation												
%	0.25	0.5	1.0	2.0	0.25	0.5	1.0	2.0	0.25	0.5	1.0	2.0
4	0.0	33.3	0.0	3.6	0.0	33.3	50.0	61.1	45.6	65.9	66.8	79.1
7	(*)	(*)	(*)	0.0	(*)	(*)	33.3	26.0	0.0	0.0	(*)	(*)
9	(*)	(*)	(*)	(*)	(*)	(*)	0.0	0.0	(*)	(*)	14.7	50.7
11	(*)	(*)	(*)	(*)	(*)	(*)	(*)	(*)	(*)	(*)	(*)	41.8

3.3. Characterization of the treated tomato fruits

3.3.1. ACIDITY, pH, SOLUBLE SOLIDS AND MATURITY INDEX

The pH, acidity, soluble solids (Brix), maturity index (MI) and weight loss (g/100 g fruit) of tomato fruits are shown in table 5.

Green fruits harvested 7 days after coating application showed a loss in acidity values and an increase in pH, as compared to the green fruits immediately after coating application (t = 0 days). This is in agreement with the progress of the ripening process on the plant. At t = 7 days, CH+T seems to stimulate the maturation process, since the fruits coated with this FFDs showed the highest value for MI, and continued at high value even after 23 days.

Allowing tomatoes to ripen on the plant for up to 23 days resulted in an increase in fruit pH and the subsequent decrease in titrable acidity. This is probably due to a loss of citric acid, a specific effect of tomato maturation, also noted by Anthon et al., (2011).

TABLE 5. pH, acidity (g citric acid/100g fruit), Brix (g soluble solids/100g fruit), maturity index (MI) and total weight loss for untreated green, treated green and ripe treated tomato fruits.

FFD	pH	Acidity	Brix	MI	Weight loss(%)
green fruit (t=0 days)					
	3.86	1.054	7.08	6.782	-
green fruit (t=7 days)					
Control	3.746(0.005) ^a	1.022(0.030) ^b	6.467(0.058) ^a	6.284(0.210) ^a	6.97(0.46) ^a
CH	3.746(0.006) ^a	1.04 (0.02) ^b	6.50(0.10) ^a	6.3(0.2) ^a	8.95(1.40) ^a
CH+T	3.95(0.02) ^d	0.915(0.073) ^a	7.167(0.153) ^c	7.723(0.896) ^b	8.46(2.46) ^a
MC	3.863(0.015) ^c	1.054(0.028) ^b	6.9(0.2) ^b	6.65(0.43) ^a	9.62(1.70) ^a
MC+T	3.826(0.015) ^b	1.087(0.014) ^b	7.30(0.10) ^c	6.634(0.252) ^a	10.8(0.6) ^a
ripe fruit (t=23 days)					
Control	4.36(0.00) ^c	0.744(0.055) ^b	3.483(0.317) ^a	4.713(0.767) ^a	8.85(0.17) ^b
CH	4.47(0.00) ^e	0.504(0.079) ^a	5.55(0.05) ^c	11.233(2.042) ^b	7.29(0.13) ^a
CH+T	4.406(0.006) ^d	0.578(0.059) ^a	5.45(0.05) ^c	9.478(0.907) ^b	8.79(0.27) ^b
MC	4.163(0.012) ^a	0.615(0.156) ^{ab}	6.15(0.15) ^d	10.429(2.529) ^b	7.66(0.64) ^a
MC+T	4.2(0.0) ^b	0.77 (0.05) ^b	4.033(0.152) ^b	5.244(0.496) ^a	7.36(0.23) ^a

Different superscripts (a, b, c and d) indicate significant differences according to ANOVA test ($p < 0.05$).

3.3.2. RESPIRATION RATE

The respiration rate (RR) in terms of oxygen consumption and carbon dioxide production of fruits harvested in green stage is shown in figure 5. The respiration quotient varied between 1.02 and 1.47 during storage. The respiration pattern of the fruits was not significantly influenced by the coatings. A maximum RR peak was noticed at 6 days of storage, which is in agreement with the climacteric behavior of tomato fruit.

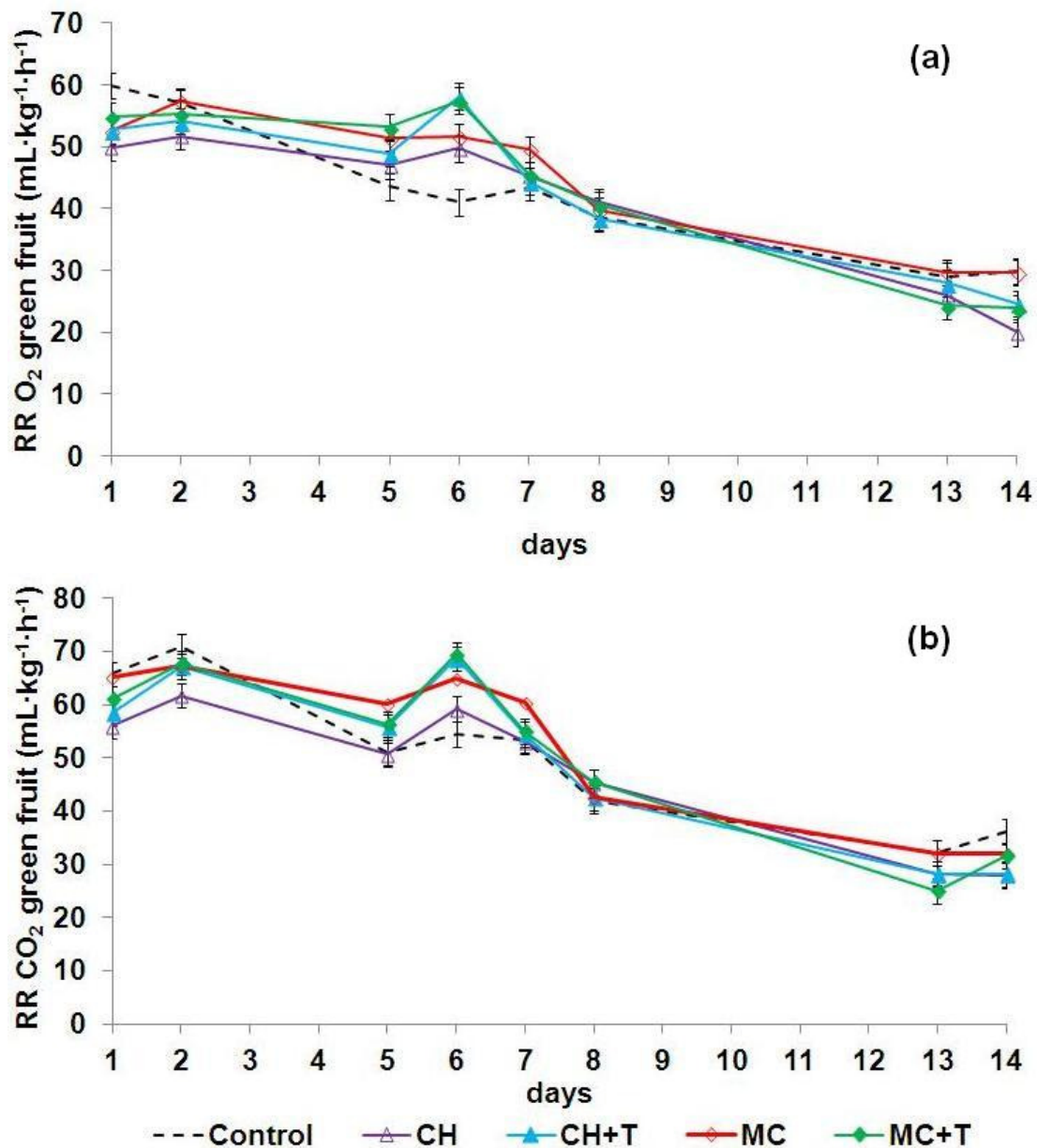


FIGURE 5. Respiration rate ($\text{mL}\cdot\text{kg}^{-1}\cdot\text{h}^{-1}$) for green-treated fruit in terms of (a) O_2 and (b) CO_2 as a function of storage time and coating formulation. 95% Fisher's LSD intervals according to ANOVA test ($n = 2$)

The respiration pattern for the fruits harvested in fully ripe stage is shown in table 6. RR decreased during the whole period of storage, in agreement with senescence of the fruit. Coatings led to some decrease in the RR with regards to the non-coated fruits during storage. There were no significant differences between samples coated with the different FFDs.

TABLE 6: Respiration rate for tomato fruits harvested in fully ripe stage. Mean values and standard deviation in brackets.

Days	RR _{O₂} (mL·kg ⁻¹ ·h ⁻¹)					RR _{CO₂} (mL·kg ⁻¹ ·h ⁻¹)				
	Control	CH	CH+T	MC	MC+T	Control	CH	CH+T	MC	MC+T
2	26.9 (8.4) ^{ax}	24.3 (1.7) ^{ax}	28.9 (3.5) ^{ax}	22.5 (0.3) ^{ax}	30.3 (7.6) ^{ax}	33.126 (11.314) ^{ax}	25.43 (0.28) ^{ax}	32.22 (8.17) ^{ax}	30.8 (3.3) ^{ax}	31.5 (0.3) ^{ax}
5	15.813 (1.070) ^{ay}	12.043 (3.603) ^{axy}	14.8 (4.8) ^{ay}	16.54 (0.12) ^{ax}	18.09 (0.18) ^{ay}	22.23 (1.89) ^{ay}	17.29 (5.26) ^{ax}	21.36 (3.89) ^{ay}	19.19 (0.14) ^{ay}	17.02 (3.75) ^{ay}
8	17.06 (0.62) ^{ay}	8.67 (0.02) ^{by}	13.3 (1.6) ^{aby}	8.8 (0.5) ^{by}	13.6 (1.2) ^{aby}	19.7 (4.4) ^{ay}	17.85 (5.86) ^{ax}	18.106 (1.845) ^{ay}	17.95 (3.74) ^{ay}	21.112 (1.77) ^{ay}
13	23.5 (1.2) ^{axy}	17.87 (1.73) ^{axy}	20.2 (1.4) ^{ay}	21.8 (10.3) ^{ax}	20.3 (1.9) ^{ay}	20.89 (2.05) ^{ay}	18.55 (1.08) ^{ax}	12.42 (2.02) ^{ayz}	18.694 (0.006) ^{ay}	13.62 (3.04) ^{ay}

Different superscripts (a, b) within a row indicate significant differences due to the coatings according to ANOVA test ($p < 0.05$). Different superscripts (x, y) within a column indicate significant differences due to time according to ANOVA test ($p < 0.05$).

3.3.3. COLOR PROGRESSION OVER STORAGE

The changes in chromatic parameters are presented in figure 4.

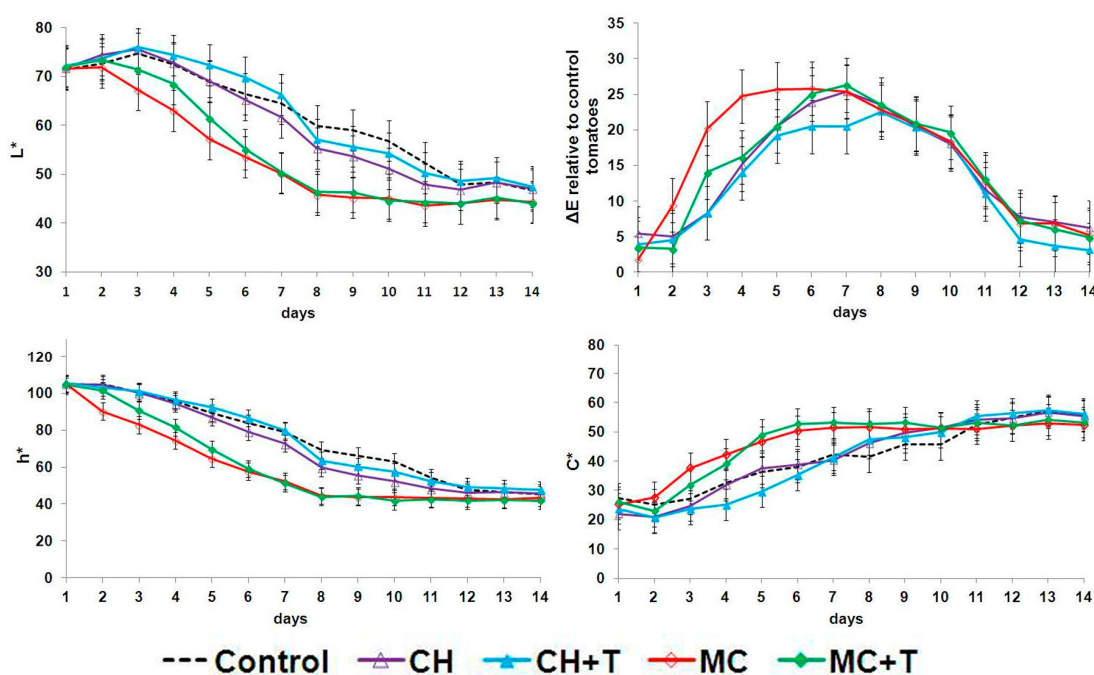


FIGURE 4. Green-treated tomato fruit lightness (L^*), hue (h^*), chroma (C^*) and color difference (ΔE) evolution in time (days). Mean values and 95% Fisher's LSD intervals according to ANOVA test ($n = 5$).

Lightness (L^*_{ab}) and hue (h^*_{ab}) values decreased during storage, which is in agreement with the ripening process and the moisture loss over time (table 5).

Samples coated with MC and MC+T ripened slightly faster (lower hue values) than the non-coated (control) and samples coated with chitosan-based FFDs.

As seen in the evolution of total colour difference (ΔE), MC coatings led to the greatest color changes as regards to the non-coated samples. From the climacterium (6 days) the color differences were not marked and all fruits presented a red hue.

4. CONCLUSIONS

Film-forming dispersions prepared with chitosan presented reduced particle sizes as compared to those that were methylcellulose-based. The type of EO influenced the final droplet size. Films without essential oil had a homogeneous structure. Chitosan-based films have shown a better integration of the oil in the matrix, coherently with their lower loss of essential oil. Moisture content and water permeability was higher in chitosan films than in those that were methylcellulose-based, coherently with the more hydrophilic character of chitosan. The addition of essential oil to both types of polymer film reduced the hydrophilic character of both types of film matrices.

In vitro antifungal activity depended on the EO proportion. Thyme and oregano were more effective than basil EO. The application of the film-forming dispersions containing thyme essential oil accelerated the progress of maturation in tomato fruits during storage. Coatings did not induce significant changes in the respiration pattern of the fruits.

5. REFERENCES

- Ahmed, J.; Al-Foudari, M.; Al-Salman, F.; Almusallam, A. S. *Effect of particle size and temperature on rheological, thermal, and structural properties of pumpkin flour dispersion*. Journal of Food Engineering 124 (2014); 43–53.
- Angelini, L.G.; Carpanese, G.; Cioni, P.L.; Morelli, I.; Macchia, M.; Flamini, G. *Essential oils from Mediterranean Lamiaceae as weed germination inhibitors*. J. Agric. Food Chem. 51 (2003); 6158-6164.
- Anthon, Gordon E; LeStrange, Michelle; Barrett, Diane M. *Changes in pH, acids, sugars and other quality parameters during extended vine holding of ripe processing tomatoes*. Wiley Online Library, (2011).
- Atarés, L., Bonilla, J., Chiralt, A. *Characterization of sodium caseinate-based edible films incorporated with cinnamon or ginger essential oils*, Journal of Food Engineering 100 (2010); 678–687.
- Bakkali, F., Averbeck, S., Averbeck, D., Idaomar, M. *Biological effects of essential oils – a review*, Food and Chemical Toxicology 46 (2008); 446–475
- Baptista, F.J.; Bailey, B.J.; Meneses, J.F. *Effect of nocturnal ventilation on the occurrence of Botrytis cinerea in Mediterranean unheated tomato greenhouses*, Crop Protection 32 (2012); 144-149.
- Garcia, Maria A.; Pinottia, Adriana; Martino, Miriam N.; Zaritzky, Noemi E.; *Characterization of composite hydrocolloid films*, Science Direct Carbohydrate Polymers 56 (2004); 339–345.

- Kim, H-J.; Chen, F.; Wang, X.; Rajapakse, N. C. *Effect of Chitosan on the Biological Properties of Sweet Basil (Ocimum basilicum L.)*, J. Agric. Food Chem. 53 (2005); 3696-3701.
- Lee, S-J; Umamo, K.; Shibamoto, T.; Lee, K-G. Identification of volatile components in basil (*Ocimum basilicum L.*) and thyme leaves (*Thymus vulgaris L.*) and *their antioxidant properties*. Science Direct, Food Chemistry 91 (2005); 131–137.
- Perdones, A.; Sanchez-Gonzalez, L; Chiralt, A; Vargas, M. *Effect of chitosan–lemon essential oil coatings on storage-keeping quality of strawberry*, Postharvest Biology and Technology 70 (2012) 32–41.
- Polder, G.; van der Heijden, G.. *Measuring Ripening of Tomatoes Using Imaging Spectrometry*, Elsevier, Hyperspectral Imaging for Food Quality Analysis and Control, (2010); chapter 12: 369-402.
- Rodríguez, M.S., Albertengo, L.A., Agulló, E. *Emulsification capacity of chitosan*, Carbohydrate Polymers 48 (2002); 271-276.
- Sánchez-González, L.; Cháfer, M.; González-Martínez, C.; Chiralt, A.; Desobry, S. *Study of the release of limonene present in chitosan films enriched with bergamot oil in food simulants*, Journal of Food Engineering 105 (2011);138–143.
- Sari, M; Biondi, D. M.; Kaâbeche, M.; Mandalari, G.; D'Arrigo, M.; Bisignano, G.; Saija, A.; Daquino, C.; Ruberto, G. *Chemical composition, antimicrobial and antioxidant activities of the essential oil of several populations of Algerian Origanum glandulosum Desf.*, Wiley InterScience flavour and fragrance journal 21 (2006); 890–898.
- Song, Y; Gao, L; Li, L; Zheng, Q. *Influence of gliadins on rheology of methylcellulose in 70% (v/v) aqueous ethanol*. Food Hydrocolloids 24 (2010); 98–104
- Turhan, K. Nazan; Sahbaz, Ferhunde; *Water vapor permeability, tensile properties and solubility of methylcellulose-based edible*, Journal of Food Engineering 61 (2004); 459–466
- Vargas, M; Albors, A; Chiralt, A; González-Martínez, C. *Water interactions and microstructure of chitosan-methylcellulose composite films as affected by ionic concentration*, LWT - Food Science and Technology 44 (2011) 2290-2295.